

Electronic Supplementary Information

Chitosan-Assisted Synthesis of 1D g-C₃N₄ Nanorods for Enhanced Photocatalysis

Yaqian Wang,^a Xiaonan Yang,^b Tong Tian,^b Yue Liu,^a Yan Chen,^a Gengsheng Xu,^b Lina Gu,^a Huiquan Li,^{c,*} Yupeng Yuan^{b,*}

^a School of Chemistry and Chemical Engineering, Anhui University, Hefei 230601, P. R. China.

^b School of Materials Science and Engineering, and Energy Materials and Devices Key Lab of Anhui Province for Photoelectric Conversion, Anhui University, Hefei 230601, P. R. China.

^c School of Chemistry and Materials Engineering, Fuyang Normal University, Fuyang 236037, P. R. China.

**Corresponding authors*

Email: huiquanli0908@163.com (Huiquan Li) ; yupengyuan@ahu.edu.cn. (Yupeng Yuan)

Experimental section

1. Reagents

Melamine (AR), triethanolamine (TEOA, AR), and chitosan((C₆H₁₁NO₄)_n, low viscosity<200 mPa.S) were purchased from Aladdin. Anhydrous ethanol (AR) and chloroplatinic acid (H₂PtCl₆·6H₂O) were purchased from Sinopharm Reagent Network. All reagents were used without any additional purification in the experiments, unless otherwise specified.

2. Synthesis of 1D g-C₃N₄ nanorods

To prepare chitosan-modified melamine, various amounts of chitosan (0.03, 0.06, 0.09, and 0.12 g) were dissolved in a mixed solution of water and ethanol (1:1). 2.0 g of melamine was then added into the chitosan solution. The mixture was vigorously stirred for 30 min and subjected to ultrasonic dispersion for additional 30 min. Subsequently, the suspension was transferred into a 100 mL Teflon autoclave and heated at 180 °C for 4 h. The resulting products were washed 3 times with ethanol and deionized water, followed by drying in an oven at 60 °C for 12 h. The samples thus obtained were labelled as C_x (x=0, 1, 2, 3, and 4, refers to the added chitosan mass of 0, 0.03, 0.06, 0.09, and 0.12 g, respectively).

Afterwards, the C_x samples were thermolyzed in a muffle furnace at 520 °C for 4 h at a heating rate of 10 °C min⁻¹. After cooling down to room temperature, the resulting products were ground into powder and labelled as CN-C_x (x=1, 2, 3, 4). For comparison, a reference sample, denoted as CN-C₀, was prepared from the thermolysis of hydrothermally pretreated melamine in the absence of chitosan. In addition, CN(C) reference sample was prepared as follows: melamine (5.0 g) and glucose (0.012 g) were placed in 100 mL beaker with 40 mL deionized water. After stirring for 30 min, the white viscous suspensions were transferred into 50 mL autoclave and heated to 180 °C for 24 h. The prepared samples were collected and washed several times with the mixed solution of ethanol and

deionized water. Finally, the C doped g-C₃N₄ was obtained by calcination at 520 °C for 2 h.

3. Characterizations

The morphology was observed on a field-emission scanning electron microscopy (FESEM, Hitachi S-4800) and a transmission electron microscopy (TEM, JEM-2100), respectively. The crystal structure was analyzed using a DX-2700 X-ray diffractometer with Cu K_α1 radiation ($\lambda = 0.1541$ nm). Fourier-transform infrared spectra (FT-IR) in the wavenumber range of 400 to 4000 cm⁻¹ were conducted on an IRPrestige-21 FT-IR spectrometer. X-ray photoelectron spectra (XPS) were measured using an ESCALAB 250Xi instrument with Al K_α radiation. The Brunauer-Emmett-Teller (BET) specific surface area and pore size distribution were determined using a physical adsorption analyser (ASAP 2020). Elemental analysis was performed on an elemental analyser (Vario EL-3). The solid-state ¹³C and ¹⁵N cross polarization magic-angle spinning (CP MAS) spectra were obtained using a Bruker Avance III 600 nuclear magnetic resonance (NMR) spectrometer at proton resonance frequencies of 150.9 (¹³C) and 60.8 MHz (¹⁵N). The UV-vis diffuse reflectance spectra (DRS) were measured on a UV-vis spectrophotometer (HITACHI U-3900). A Bruker EMXnano spectrometer was employed to monitor the electron paramagnetic resonance (EPR) signal at room temperature. Photoluminescence (PL) spectra and time-resolved photoluminescence (TR-PL) spectra were conducted on a fluorescence spectrophotometer (HITACHI F-4500) and a spectrometer (Horiba Fluoro max plus), respectively.

4. Photoelectrochemical tests:

Electrochemical measurements of electrochemical impedance spectra (EIS), linear sweep voltammetry curves (LSV), Mott-Schottky plots, and transient photocurrent responses were carried out on an electrochemical workstation (Chenhua CHI-660E) in a standard three-electrode cell. The reference electrode, counter electrode, and working electrode are Ag/AgCl (containing saturated KCl solution), platinum (Pt) foil, and catalyst-coated fluorine-doped tin oxide (FTO), respectively. The electrolyte is 0.5 M Na₂SO₄ solution. The working electrode was prepared as follows: First, 5 mg of photocatalyst was dispersed in 0.5 mL of 0.5 wt.% Nafion solution under ultrasonic treatment for 30 min. Afterward, the obtained slurry was drop-coated onto an FTO conductive glass (1 cm x 1 cm) to prepare the working electrode. A 300W Xe lamp with a 420 nm cut-off filter was used to provide the visible light ($\lambda \geq 420$ nm), which was manually chopped during the measurements of photocurrent response. Mott-Schottky plots were also measured under the visible light irradiation ($\lambda \geq 420$ nm). For EIS spectra, the frequency range was set from 1 to 10⁶ Hz and the bias was set to -0.5 V.

5. Photocatalytic hydrogen generation:

Photocatalytic H₂ generation was tested in a 70 mL Pyrex reactor under visible light irradiation. Typically, 20 mg of photocatalysts was dispersed into a 20 mL of 10 wt.% TEOA solution, and then a 106 μ L of H₂PtCl₆·6H₂O solution (0.98 g/L) was added to this suspension as the source of 0.2 wt.% Pt co-catalyst. The reactor was sealed and then bubbled with Ar for 15 min to remove residual air. Afterwards, the reactor was irradiated by a 300 W Xe lamp with a 420 nm cut-off filter ($\lambda \geq 420$ nm) to provide visible light. The light intensity is measured to 560.5 mW cm⁻² by using a power meter (Newport 1918-R). Under magnetic stirring, the gas products were analysed using a gas chromatograph (GC-1690, Kexiao) equipped with a thermal conductive detector (TCD), and Argon was used as the carrier gas.

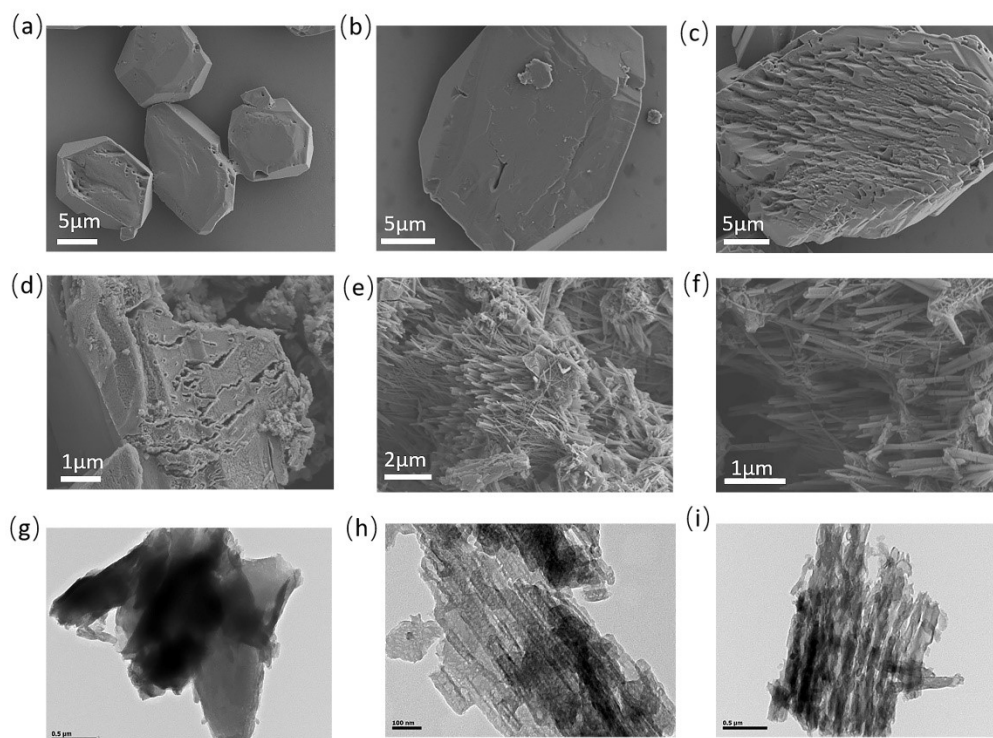


Fig. S1 SEM images for (a) pristine melamine, (b) C₀, (c) C₃, (d) CN-C₀, (e) CN-C₃, (f) magnified CN-C₃. TEM images of (g) CN-C₀, (h) and (i) CN-C₃.

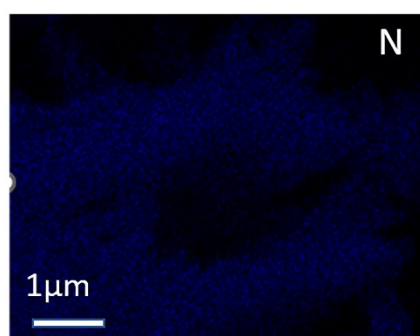
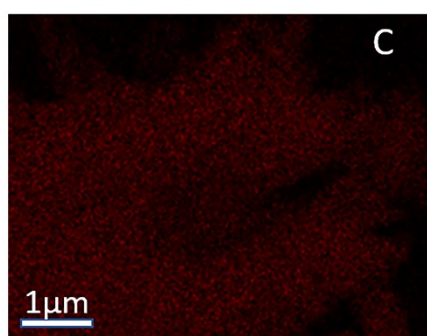
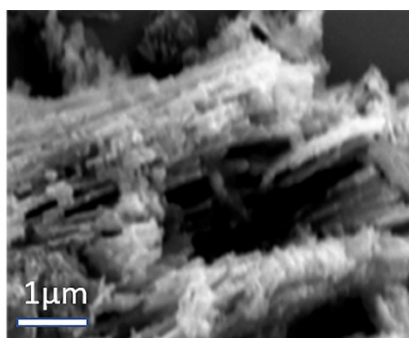


Fig. S2 TEM bright-field image (upper panel), elemental mapping of CN-C₃ for C and N elements.

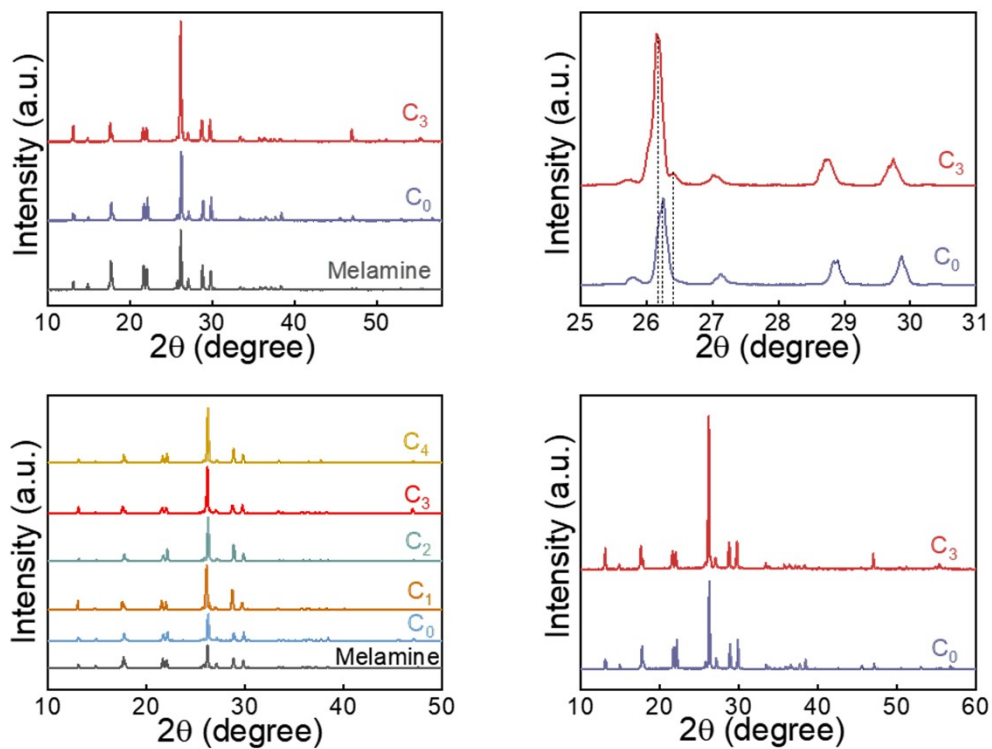


Fig. S3 XRD patterns of precursor C_x .

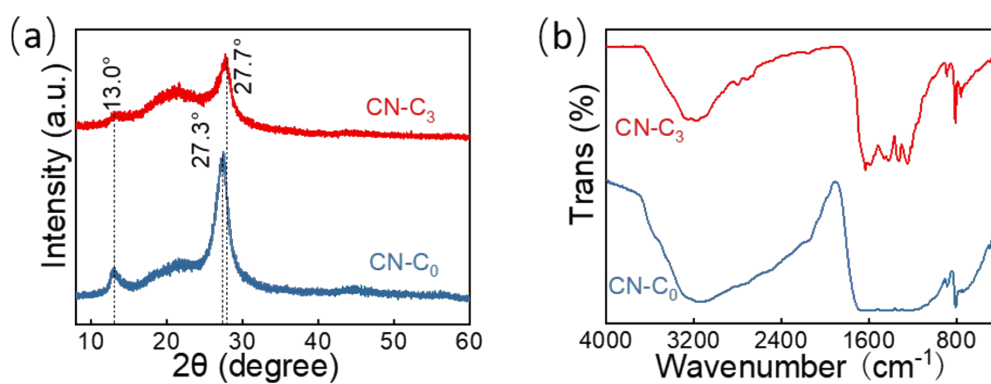


Fig. S4 (a) XRD patterns, (b) FT-IR spectrum of CN- C_0 and CN- C_3

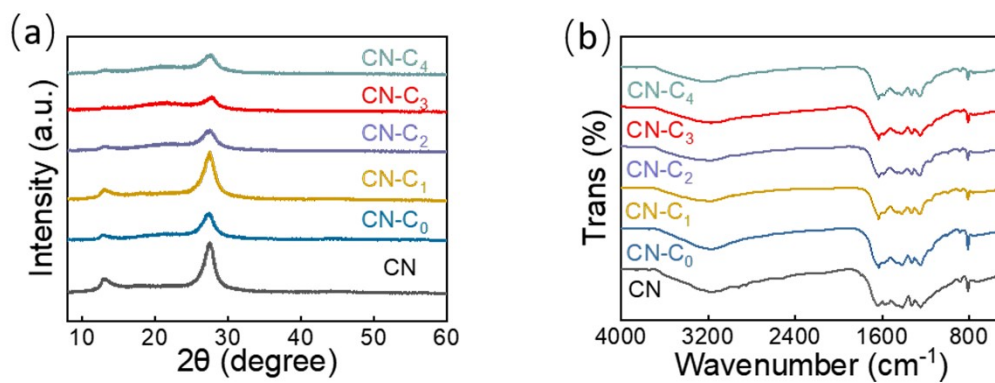


Fig. S5 (a) XRD patterns and (b) FT-IR spectra for CN-C_x and CN-C_x samples.

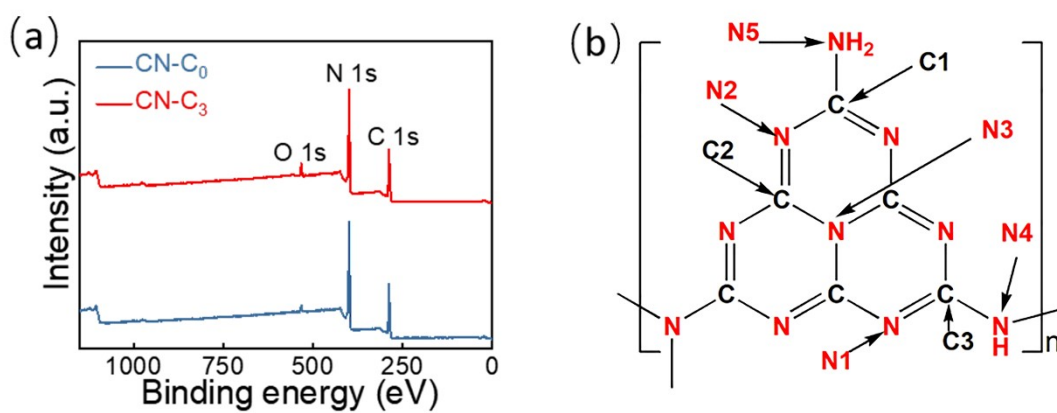


Fig. S6 (a) XPS survey scan of CN-C₃ and CN-C₀ sample. (b) the C and N positions in heptazine unit.

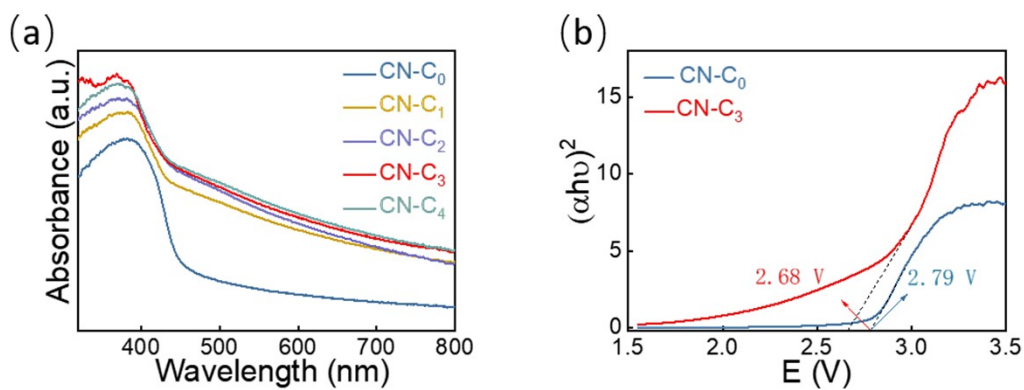


Fig. S7 (a) UV-vis DRS spectra of CN-C_x. (b) The Tauc plots of CN-C₃ and CN-C₀ sample.

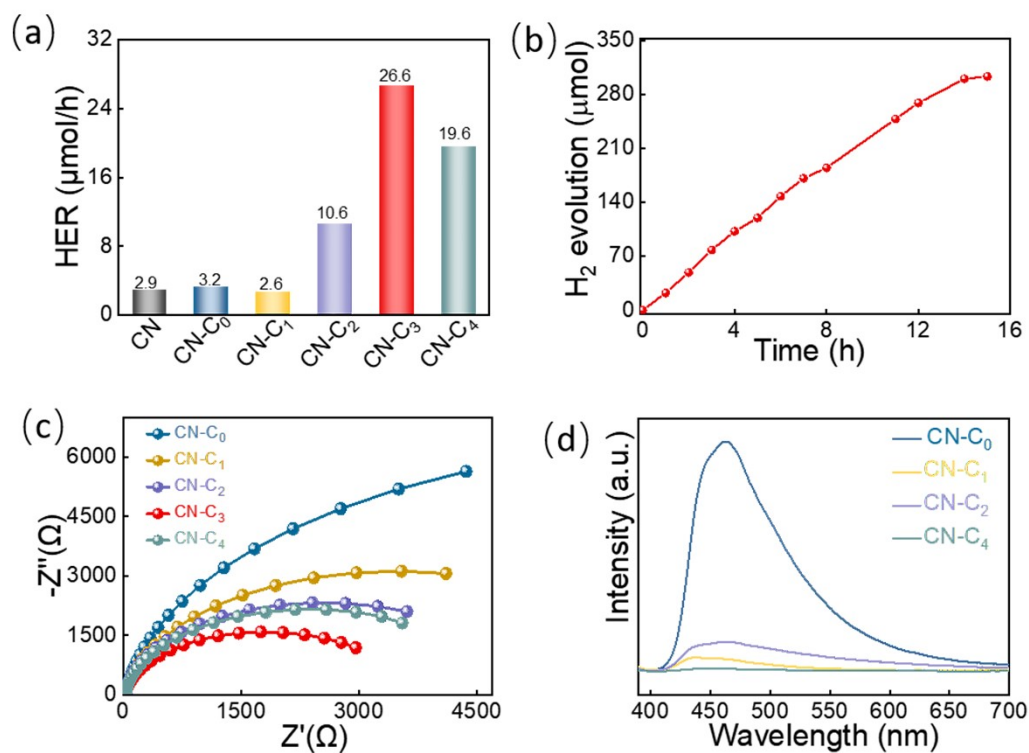


Fig. S8 (a) H₂ generation rate of CN-C_x and CN samples. (b) Long-term H₂ generation of CN-C₃ sample. (c) EIS spectra and (d) Steady-state PL spectra of CN-C_x.

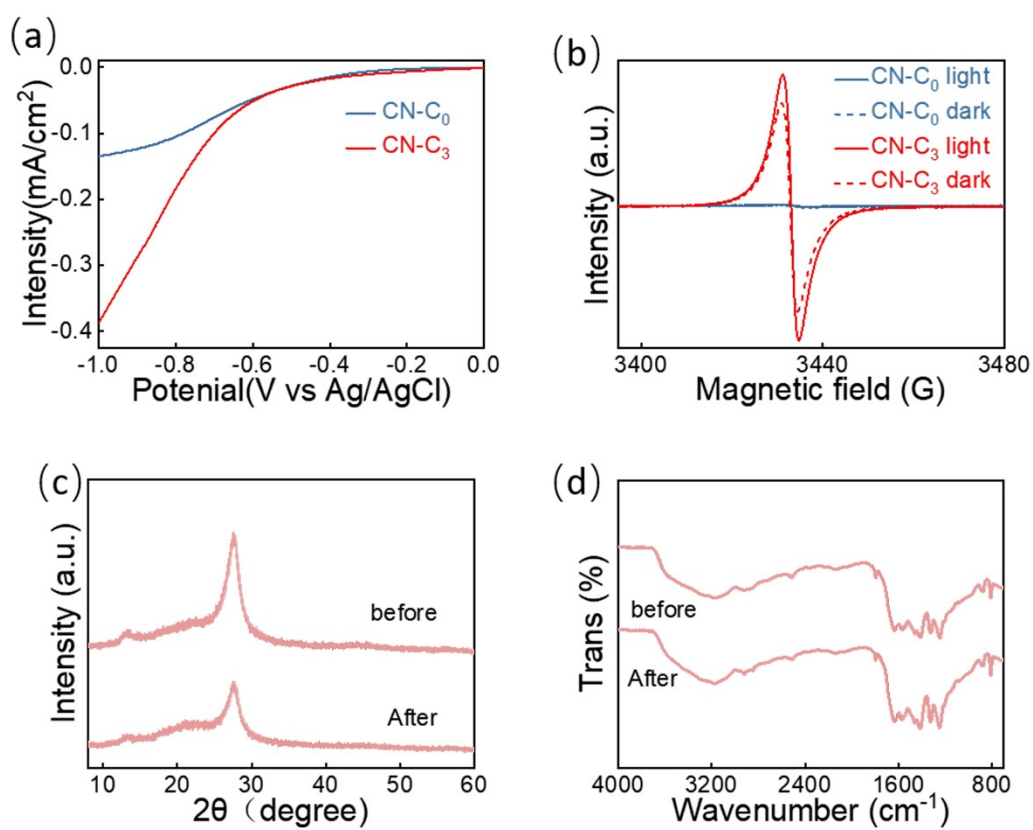


Fig. S9 (a) LSV curves of CN-C₃ and CN-C₀ samples. (b) Low-temperature EPR spectra of CN-C₃ and CN-C₀ samples recorded in the dark and under visible light irradiation. (c) XRD patterns and (d) FT-IR spectra of CN-C₃ before and after photocatalytic hydrogen evolution tests.

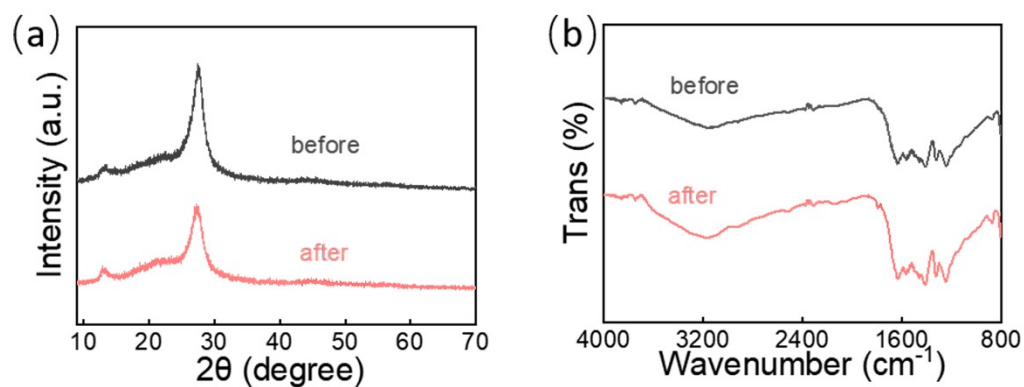


Fig. S10 (a) XRD patterns and (b) FT-IR spectra of CN-C₃ before and after 24 hours of photocatalytic hydrogen evolution tests.

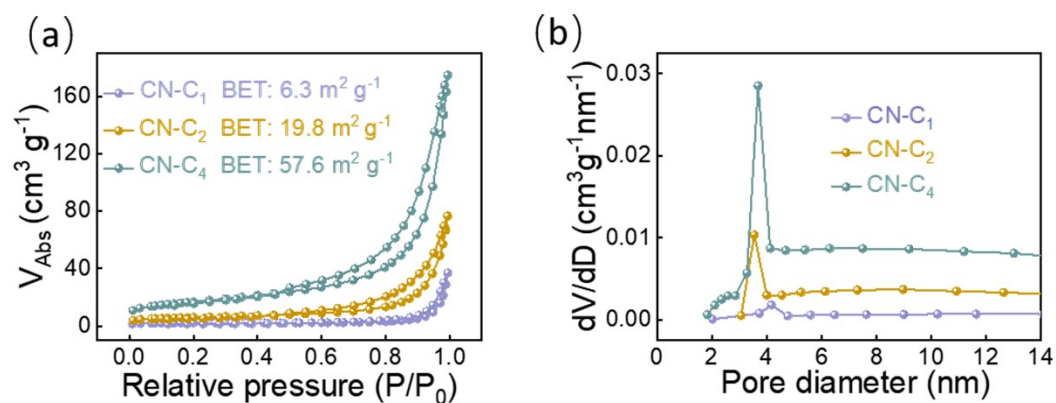
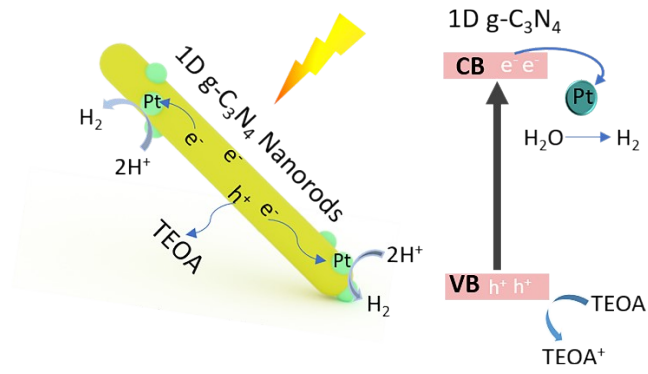


Fig. S11 (a) N_2 absorption–desorption isotherms and (b) the corresponding pore size distribution of CN-C₁, CN-C₂ and CN-C₄ sample.



Scheme 1. Proposed mechanism for photocatalytic H₂ generation over CN-C sample.

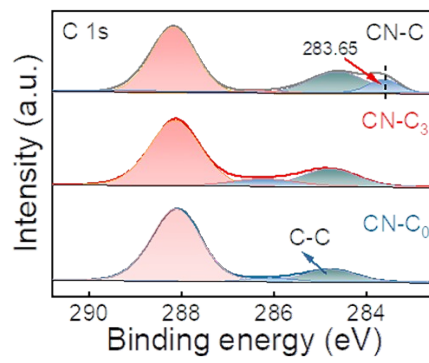


Fig. S12 High-resolution XPS spectra of C 1s for CN-C₀, CN-C₃ and CN-C sample.

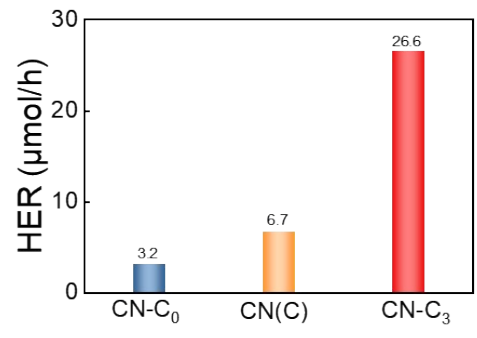


Fig. S13 H₂ generation rate of CN-C₀, CN-C₃, and CN(C).